Turkish J. Eng. Env. Sci.
32 (2008) , 295 – 302.

Investigation and Analysis of Ogive-Shape Nose Steel Projectile into Concrete Target

Khodadad VAHEDI, Mohammad LATIFI
Department of Mechanical Engineering, Imam Hossein University, Tehran-IRAN
e-mail: mh.latifi@gmail.com
Ferydoon KHOSRAVI
Department of Civil Engineering, Imam Hossein University, Tehran-IRAN

Received 27.06.2008

Abstract

Penetration of projectile into concrete target is of high interest to both civilian as well as applied scientists. The penetration process is highly complex and due to it interdisciplinary nature, most of the works in this respect are experimental. High cost of experimentation has forced many of the investigators to rely on simple analytical and engineering models. Recent investigations rely heavily on simulation processes using available software tools.

The aim of this paper is to simulate the penetration of a high velocity ogive-shape nose steel projectile into concrete target. The crater depth is also obtained using analytical formula developed by Forrestal. The results of the analytical as well as LS-DYNA simulation are compared with the experimental results of valid sources and a very good agreement is recorded.

Key Words: Penetration, Projectile, Cavity expansion, Concrete, LS-DYNA.

Introduction

Concrete has been used as a main constituent in the structure of tunnels, bridges, and nuclear reactors. In the past century most of the work has relied heavily on experimentation. These experiments covered several different projectile shapes including ogival, spherical, sharp nose, and cylindrical projectiles.

Several empirical relations to predict penetration depth, deduced from experimental studies, have been summarized by Kennedy (1997), and their range of validity has been delineated. Yankelevsky (1997) analyzed the local response of concrete slabs to low speed missile impact and compared his results with those predicted by formulas proposed by Petry.

All of these relations were based on curve fits to experimental data, predicted one parameter as a function of others, and did not account for any local material response. Yankelevsky (1997) observed significant variations in predictions from these relations.

The development of analytical penetration models that accounted for the material behavior began in the 1940s with equations predicting the penetration of steel targets by metallic rods. Bishop et al. (1945) studied quasi-static expansions of cylindrical and spherical cavities and used them to estimate forces on conical nose punches into metallic targets.

Forrestal (1986) used the cylindrical cavity expansion theory to study the penetration of rigid rod into dry porous rock and showed that they overpredict the early time deceleration response and under-predict the later deceleration response.

Forrestal and Luk (1992) also showed that the deceleration predictions from the spherical expansion approximation were in good agreement with the experimental results. Forrestal et al.(1995) and Tzou et al. (1997) generalized these models to predict penetration depth into metallic and concrete targets, respectively.

Numerical and experimental adaptations to the cavity expansion based methods have been given by Warren et al. (2004) and Gomez and Shukla (2001). Warren used finite element method (FEM) to analyze the penetration problem. He simulated concrete's response as strain hardening and pressure dependent yield strength and accounted for pore collapse.

Agardh and Laine (1999) conducted a 3-dimensional (3-D) simulation of a high-speed solid steel cylinder impacting and perforating a RC slab whose thickness equaled approximately twice the penetrator length.

We add that Warren and Poorman (2001) have recently examined, experimentally and numerically, the effect of obliquity on the penetration of the projectiles with emphasis on the bending of the projectile and its trajectory. A good agreement between test and simulation result was obtained.

Huang et al.(2005) used LS-DYNA modeling to investigate the perforation of a reinforced concrete target and compared their results with experimental data presented by Hanchak and published their results.

Tham et al. (2006) investigated the penetration depth of an ogive-nose projectile penetrating into a concrete target using AUTODYN-2D and compared their findings with experimental results.

The purpose of this study is to simulate the penetration of a high velocity ogive–nose shape steel projectile into semi-infinite concrete target. Experimental data were used to validate the simulation process. At the same time penetration depth into concrete target was calculated using analytical formula developed by Forrestal (1993). These 2 approaches are then compared with the experimental data and the results are presented.

Constitutive model

In this study the penetration of an ogive-nose shape steel projectile into a semi-infinite concrete target is simulated. In order to obtain the desired result of simulation, selection of the constitutive model and the precision of the inputs are of high importance.

The constitutive models used for the steel projectile and concrete are Simplified Johnson Cook and Johnson Holmquist, respectively; these constitutive models are described briefly.

Johnson Holmquist model

As mentioned previously, the model used in this article to simulate concrete target is the Johnson Holmquist model (Holmquist et al., 1993; Johnson 1998). The model can be used to simulate concrete target under high strain rates and pressure. Strength of the concrete in this model is expressed as a function of pressure, strain rate, and damage. Also pressure is expressed as a function of volumetric strain and includes the effect of permanent deformation change. Damage is modeled as a function of volumetric plastic strain, equivalent plastic strain, and pressure (Shiou Tai and Chin Tang, 2006).

Based on this model normalized equivalent stress is defined as:

$$\sigma^* = \frac{\sigma}{f'_c} \tag{1}$$

In Eq. (1), σ is the actual equivalent stress and f'_c is the quasi–static uniaxial compressive strength.

Referring to Figure 1(a), σ^* for concrete is determined from:

$$\sigma^* = \left[A(1-D) + BP^{*N'}\right].[1 + C\ln\dot{\varepsilon}^*] \tag{2}$$

In Eq. (2) normalized pressurep^* is defined as $p^* = \frac{p}{f'_c}$ and $\dot{\varepsilon}^*$ is the dimensionless strain rate given as: $\dot{\varepsilon}^* = \frac{\dot{\varepsilon}}{\dot{\varepsilon}_0}$.

Here $\dot{\varepsilon}$ is the actual strain rate, $\dot{\varepsilon}_0 = 1s^{-1}$ is the reference strain rate, and D is the damage parameter ($0 \le D \le 1$). Also, A is the normalized cohesive strength, B is normalized compressive stiffness coefficient, N' is pressure hardening exponent, C is strain rate coefficient, and $\sigma^*_{\max}$ is normalized maximum strength of concrete.

The damage considered for the element in the Johnson Holmquist model is similar to Johnson Cook. The difference is that in Johnson Holmquist model, volumetric plastic strain for the calculation of damage is also considered (Figure 1(b)).

In order to calculate the damage to the element, the following equation is used:

$$D = \sum \frac{\Delta\varepsilon_P + \Delta\mu_P}{D_1(P^* + T^*)^{D_2}} \tag{3}$$

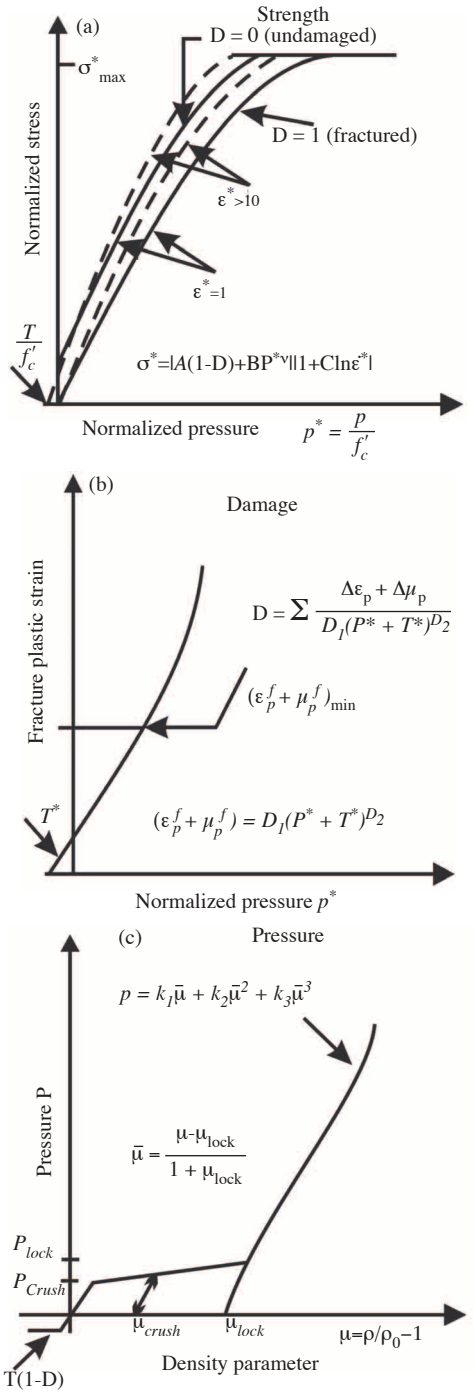

Figure 1. Concrete material models: (a) Equivalent strength model, (b) Damage failure model, (c) Equation of state (Holmquist et al. 1993).

In Eq. (3) $\Delta\varepsilon_p$ is the equivalent plastic strain increment. D_1 and $D_2$are damage constants of the material. T^* is the normalized maximum tensile strength given by $T^* = \frac{T}{f_c'}$.

In order to calculate pressure in Johnson Holmquist model, according to Figure 1(c) using the assumption of compressible material, an equation of the following form is used:

$$p = k_1\bar{\mu} + k_2\bar{\mu}^2 + k_3\bar{\mu}^3 \tag{4}$$

In Eq. (4) k_1, k_2, and k_3 are constants and $\bar{\mu}$ is the volumetric strain given by:

$$\bar{\mu} = \frac{\mu - \mu_{lock}}{1 + \mu_{lock}} \tag{5}$$

Where, μ_{lock} is the volumetric plastic strain.

The parameters used in Johnson Holmquist model and their values are presented in Table 1.

Table 1. The material parameters of the concrete (Shiou Tai and Chin Tang, 2006).

Numerical Values	Material Properties	Numerical Values	Material Properties
1	D_2	2300	$\rho(kg/m^3)$
0.01	$EF_{\min}$	13567	$G(MPa)$
13.6	$P_{crush}(MPa)$	51	$f_c'(MPa)$
0.00058	μ_{crush}	0.75	A
17.4	$k_1(GPa)$	1.65	B
38.8	$k_2(GPa)$	0.76	N'
29.8	$k_3(GPa)$	0.007	C
1.05	$P_{lock}(MPa)$	11.7	$\sigma^*_{\max}$
0.1	μ_{lock}	0.03	D_1

Simplified Johnson Cook model

As noted previously, the model considered for the projectile material in this article is the Simplified Johnson Cook model. This material model is similar to Johnson Cook but the difference is that the effects of the temperature and damage are not considered. This will cause an increase in the speed of calculation by 50% (Hallquist, 2003). The experiments performed by Forrestal et al., (1993) indicate that mass erosion for the projectile velocity from 400 to 800 m/s is less than 5% of the projectile mass and therefore simplified Johnson Cook model is very effective in simulation process. Also this material model is a good candidate for the shell elements.

Here, the stress is calculated using the following relation (Hallquist, 2003):

$$\sigma_y = (R_1 + R_2\bar{\varepsilon}_P)(1 + R_3 \ln \dot{\varepsilon}^*) \tag{6}$$

whereR_1,R_2,R_3 are constants and $\dot{\varepsilon}^*$ is the normalized effective plastic strain given by:

$$\dot{\varepsilon}^* = \frac{\dot{\bar{\varepsilon}}_P}{\dot{\varepsilon}_0} \tag{7}$$

It is also noted that $\dot{\varepsilon}_0 = 1s^{-1}$.The numerical values considered for the parameters used in the model are presented in Table 2.

Table 2. Parameters used for annealed steel (Ballew, 2004).

Material Properties	Numerical Values
$\rho(kg/m^3)$	7840
$E(GPa)$	200
ν	0.3
$R_1(MPa)$	792.2
$R_2(MPa)$	5095
R_3	0.014

Description of the model

Experiments performed by Forrestal et al. (1995) used ogive-nose shape steel projectile with a mass of 1.6 kg and projectile nose caliber $\psi = 3$ (dimensionless parameter). The projectile penetrated into cylindrical concrete with a diameter of 0.91 m, and mean compressive pressure of 51 MPa.

Figure 2 shows the characteristics of the projectile considering the symmetrical nature of projectile and target, and in order to reduce the volume of calculation, axi-symmetric shell elements were used.

As shown in Figure 3, this analysis employed 72,296 elements and 73,096 nodes for simulation process.

The contact situation between the projectile and target are surface to surface.

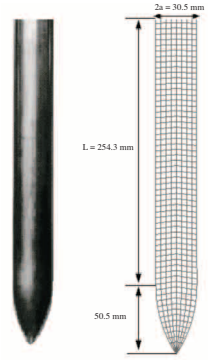

Figure 2. Specification of simulated projectile in **LS-DYNA**.

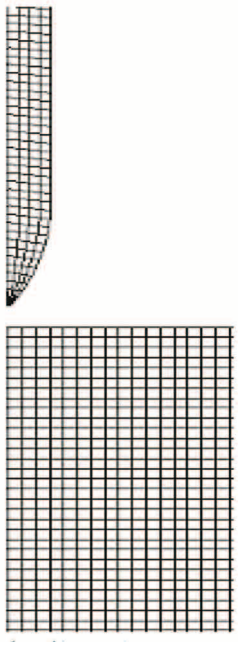

Figure 3. Projectile and target mesh in **LS-DYNA**.

In order to determine boundary condition, the nodes existing on external surface of the target were constraint in all directions, and the nodes on symmetric-axis were constraint using symmetrical nature.

Analytical relations

Forrestal et al. (1993) developed an analytical formula to calculate the penetration depth of a rigid projectile into concrete target. According to this model, as the projectile penetrates into concrete target, cavity and tunnel regions will be formed in the target. The cavity region is approximately 4 times the radius of the projectile. Here, in cavity region penetration into target is due to the surface effect. The tunnel region starts from the end of the cavity and continues up to the final penetration depth. Here, spherical cavity expansion theory, developed by Bishop (1945) and later used by Forrestal et al. (1987; 1993) to calculate normal stress on the nose of the projectile, was used to calculate the force exerted on the nose of the projectile. Now, using the model presented by Forrestal (1993; 2003), the final crater depth in concrete can be calculated.

Figure 4 shows the cavity and tunnel regions in the concrete target. Since acceleration of projectile is considered linear, axial force on the nose of the projectile in cavity region is estimated as:

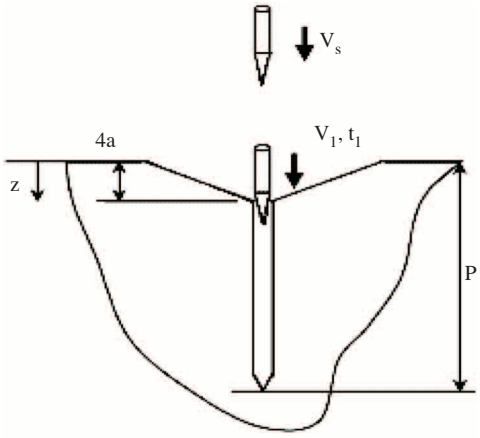

Figure 4. Cavity and tunnel region in a concrete target.

$$F = cz \tag{8}$$

where z is the displacement and c is a constant, which can be calculated using the continuity concept of velocity, displacement and force when projectile enters tunnel.

The force exerted on the projectile nose in the tunnel region using spherical cavity expansion theory is estimated as:

$$F = \pi a^2 (S f'_c + N \rho V^2) \tag{9}$$

$$N = \frac{8\psi - 1}{24\psi^2} \tag{10}$$

where S is an experimental constant depending on the compressive strength of concrete, f'_c is the concrete compressive strength, ρ is the density of the concrete, and V is the instantaneous projectile velocity, and ψ is projectile nose caliber.

Using Newton's second law and integrating Eqs. (8) and (9) in cavity and tunnel region will result into:

In cavity region

$$Z = (\frac{V_S}{\omega}) \sin \omega t \tag{11}$$

$$V = V_S \cos \omega t \tag{12}$$

$$\omega = \sqrt{\frac{c}{m}} \tag{13}$$

$$\omega = \sqrt{\frac{V_S^2 - V_1^2}{16a^2}} \tag{14}$$

In the above equation, a is the projectile radius, m is the projectile mass, V_S is the impact velocity, and V_1 is the entrance velocity from cavity to tunnel.

V_1 can be expressed as:

$$V_1 = \sqrt{\frac{m v_s^2 - 4\pi a^3 S f'_c}{m + 4\pi a^3 N \rho}} \tag{15}$$

Also time required for the projectile to pass the cavity region is:

$$t_1 = \frac{\cos^{-1}(\frac{V_1}{V_S})}{(\frac{c}{m})^{1/2}} \tag{16}$$

In tunnel region

$$W = tan^{-1} \left[(\frac{N\rho}{S f'_c})^{1/2} V_1 \right] \tag{17}$$

$$z = \frac{m}{\pi a^2 N \rho} \ln \left[\frac{\cos \left\{ W - \frac{\pi a^2}{m} (S f'_c N \rho)^{1/2} (t - t_1) \right\}}{\cos \{W\}} \right] + 4a \tag{18}$$

$$V_z = (\frac{S f'_c}{N\rho})^{1/2} \tan\{W - \frac{\pi a^2 (S f'_c N \rho)^{1/2} (t - t_1)}{m}\} \tag{19}$$

Assuming that projectile enters tunnel region of the concrete target, final penetration depth is calculated as:

$$p = \frac{m}{2\pi a^2 \rho N} \ln(1 + \frac{N\rho {V_1}^2}{S f'_c}) + 4a \tag{20}$$

Table 3 Shows the numerical values used in the analytical formula.

Table 3. Numerical values used in the analytical formula.

Analytical Parameter	Numerical Values
m(kg)	1.6
$2a(mm)$	30.5
ψ	3
$\rho(kg/m^3)$	2300
$f'_c(MPa)$	51
S	10.5

Results and Discussion

Table 4 shows the experimental results and the results of the simulation as well as the analytical formula developed by Forrestal. The results of the experiment and simulation in the present study, in velocity range of 405 to 651 m/s, are very close and the maximum error is less than 5%. This indicates that simulation process can be used with a good degree of confidence to calculate penetration depth of a rigid projectile into concrete target.

Table 4. Comparison of experimental results with simulated and analytical results.

Simulated Penetration Depth (m)	Analytical Penetration Depth (m)	Experimental Penetration Depth (m)	Impact Velocity (m/s)
0.35	0.354	0.37	405
0.4	0.42	0.42	446
0.54	0.6	0.56	545
0.75	0.8227	0.78	651

Figure 5 shows the comparison of experimental penetration depth with simulation as well as the results extracted from the analytical formula. Where velocities are less than 500m/s, the results are very close; however, at velocities higher than 500m/s, the difference between simulation and experimental results increases, which may be due to the fact that Forrestal has not taken into account the projectile nose deformation. Figure 5 also show that the calculated and simulated penetration depths are the upper and lower limits of the experimental results, respectively. This makes it possible to optimize the design of a penetrator into concrete target using the results of the analytical formula as well as the simulation-process.

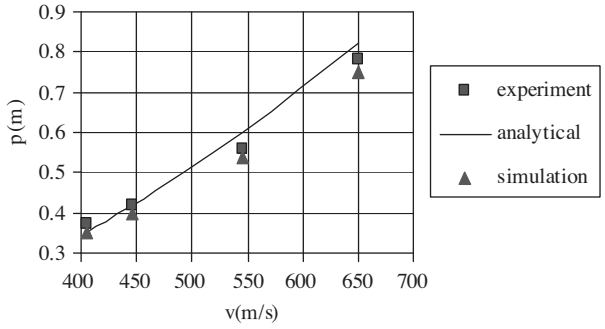

Figure 5. Comparison of experimental, analytical and simulated results.

Figures 6 and 7 show the comparison between results of the analytical formula and simulation of displacement and velocity of the projectile with respect to time. Velocity ranges in Figures 6a to 6d and Figures 7a to 7d are 405, 446, 545, and 651m/s. Close investigation of the these figures reveal a very good agreement between the simulated and analytical results.

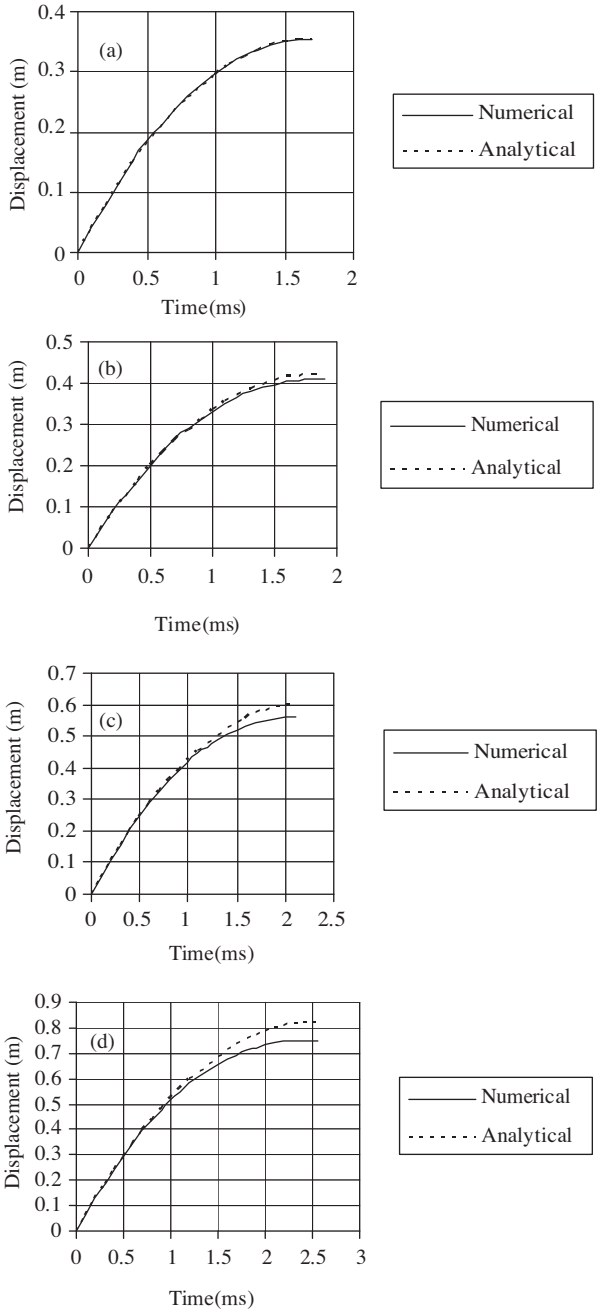

Figure 6. Comparison of numerical and simulated displacement.

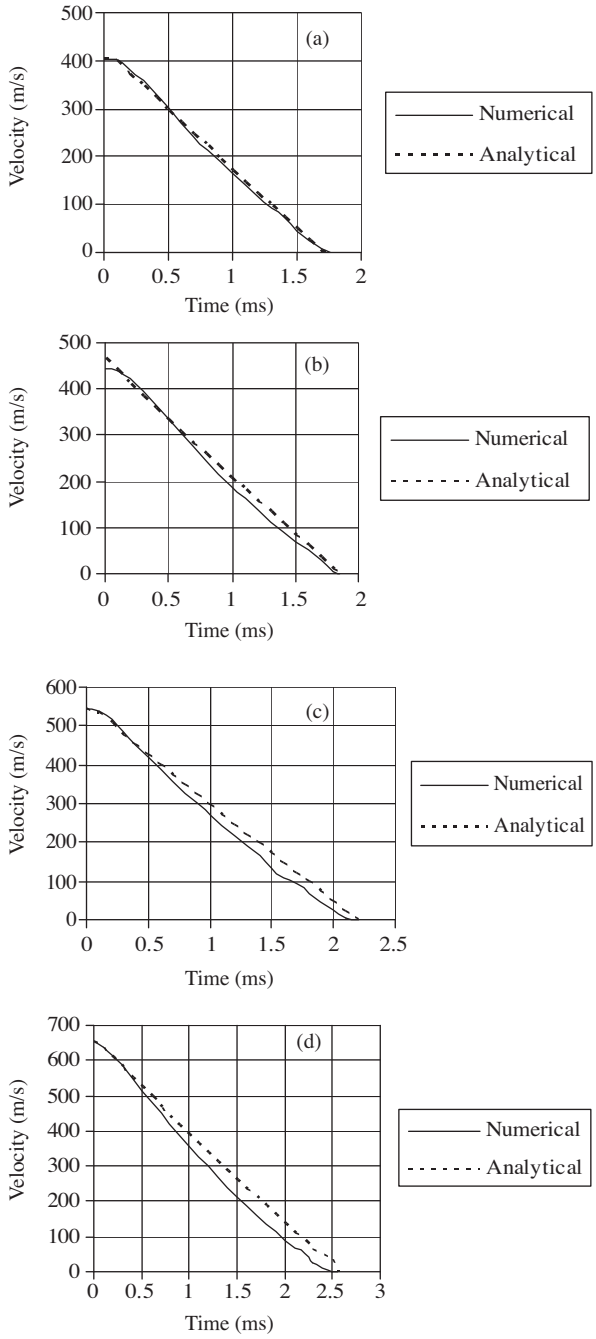

Figure 7. Comparison of numerical and simulated velocity.

As impact velocity increases, there exists a difference between analytical and simulated results, which is in close agreement with the penetration depth obtained from these methods.

Also plots of displacement and velocity with respect to time show that as projectile velocity decreases the slope of displacement in terms of time decreases substantially, which delineates the importance of impact velocity.

Conclusion

In this article an ogive-nose shape steel projectile penetrating into a semi-infinite concrete target was simulated. The results of the simulation were compared with the analytical formula presented by Forrestal and also experimental results of Ref. (Forrestal, 1995). The results of the comparison showed that a very close agreement does exist between simulation, analytical calculation, and experimental results.

It was also shown that Johnson Holmquist model can be used with sufficient accuracy to describe concrete response under large deformation.

Nomenclature

A	normalized cohesive strength
a	projectile radius (mm)
B	normalized compressive stiffness coefficient
C	strain rate coefficient
c	dimensionless constant
D, D_1, D_2	damage parameter
E	Young's modulus (GPa)
F	axial force (N)
f'_c	compressive strength (MPa)
k_1, k_2, k_3	constant (GPa)
N'	pressure hardening exponent
P	pressure (MPa)
p^*	normalized pressure
R_1, R_2	constant (MPa)
R_3	dimensionless constant
S	experimental constant
T^*	normalized maximum tensile strength
T	maximum tensile strength (MPa)
t	time (s)
t_1	time required for the projectile to pass the cavity region (s)
V_S	impact velocity (m/s)
V_1	entrance velocity from cavity to tunnel (m/s)
W	dimensionless constant
z	displacement (m)

Greek Letters

σ_y	yield stress (MPa)
$\sigma*$	normalized equivalent stress
σ	actual equivalent stress (MPa)
$\sigma^*_{\max}$	normalized maximum strength
$\bar{\varepsilon}_P$	effective plastic strain
$\Delta\varepsilon_p$	equivalent plastic strain increment
$\dot{\varepsilon}^*$	dimensionless strain rate
$\dot{\varepsilon}_0$	reference strain rate (s^{-1})
$\dot{\bar{\varepsilon}}_P$	effective plastic strain rate (s^{-1})
μ	volumetric strain
μ_{lock}	volumetric plastic strain
ν	Poisson's ratio
ρ	density (kg/m^3)
ψ	projectile nose caliber

References

Agardh, L. and Liane, L., "3D FE-Simulation of High-Velocity Fragment Perforation of Reinforced Concrete Slabs", Int. J. Impact Engng., 22, 911-922, 1999.

Bishop, R.F., Hill, R., Mott, N.F., "The Theory of Indentation and Hardness Tests", Proceeding of the Physical Society 57, Part 3, 147-155, 1945.

Ballew, W., "Taylor Impact Test and Penetration of Reinforced Concrete Targets By Cylindrical Composite Rods", Thesis for Degree of Master of Science, Virginia Polytechnic Institute and State University, 2004.

Forrestal, M.J., "Penetration Into Dry Porous Rock", Solid Struct., 22(12), 1485-1500, 1986.

Forrestal, M.J., Luk, V.K., "Penetration into Soil Targets", Int. J. Impact Engng., 12, 427-444, 1992.

Forrestal, M.J., Frew, D.J., Hanchak, S.J. and Brar, N.S., "Penetration of Grout and Concrete Targets With Ogive-Nose Steel Projectiles", Int. J. Impact Engng., 465-476, 1995.

Forrestal, M.J. and Tzou, D.Y., "A Spherical Cavity-Expansion Penetration Model for Concrete Targets", Int. J. Solids and Structures, 34, 4127-4146, 1997.

Forrestal, M.J., Altman, B.S., Cargile, J.D. and Hanchak, S.J., "An Empirical Equation for Penetration Depth of Ogive-Nose Projectiles Into Concrete Targets", Int. J. Impact Engng., 395-405, 1993.

Forrestal, M.J., Frew, D.J., Hickerson, H.P., Rohwer, T.A., "Penetration of Concrete Targets with Deceleration Time measurements", Int. J. Impact Engng., 28, 479-497, 2003.

Gomez, J.T. and Shukla, A., "Multiple Impact Penetration of Semi-Infinite Concrete", Int. J. Impact Engng., 25, 965-979, 2001.

Huang, F., Wu, H., Jin, Q. and Zhang, Q.A ., "Numerical Simulation on the Perforation of Reinforced Concrete Targets", Int. J. Impact Engng., 32, 173-187, 2005.

Holmquist, T.J., Johnson, G.R., Cook, W.H., "A Computational Constitutive Model for Concrete Subjected to Large Strains, High Strain Rates, High Pressure", The 14th international Symposium on Ballistics, Qucbec, 591-661,1993.

Hallquist, J.O., "LS-DYNA Theoretical Manual v.970, Livermore Software Technology", Corpration, Livermore CA,USA, 2003.

Johnson, G.R., "Computed Radial Stresses In A Concrete Target Penetraed by a Steel Projectile" Proceedings of the 5^{th} International Conference on Structures under Shock and Impact, Greek, 793-806, 1998.

Kennedy, R.P., "A Review of Procedures for the Analysis and Design of Concrete Structures to Resist Missile Effects", Nuclear Engineering and Design, 37, 183-203, 1976.

Luk, V.K., Forrestal, M.J., "Penetration Into Semi-Infinite Reinforced Concrete Targets With Spherical and Ogival Nose Projectiles", Int. J. Impact Engng., 6, 291-301, 1987.

Tham, C.Y., "Numerical and Empirical Approach In Predicting of a Concrete Target by an Ogive-Nosed Projectile", Int. J. Finite Element in Analysys and Dsign., 42, 1258-1268, 2006.

Tai, Yuh-Shiou and Tang, Chia-Chin, "Numerical simulation: The dynamic behavior of reinforced concrete plates under normal impact", Int. J. Theoretical and applied fracture mechanics, 117-127, 2006.

Warren, T.L., Fossum, A.F., Frew, D.J. "Penetration Into Low-Strength (23MPa) Concrete Target Characterization and simulation", Int. J. Impact Engng., 30, 477-503, 2004.

Warren, T.L. and Poorman, K.L., "Penetration of 6061-T6511 Aluminum Targets by Ogive Nosed V AR 4340 Steel Projectiles at Oblique Angles: Experiments and Simulations", Int. J. Impact Engng., 30, 477-503, 2004.

Yankelevsky, D.Z., "Local Response of Concrete Slabs to Low Velocity Missile Impact", Int. J. Impact Engng., 19, 331-343, 1997.